Scaling Parameters of the Lewis-Kostiakov Water Infiltration Equation Across Soil Textural Classes and Extension to Rain Infiltration

L. R. Ahuja, J. A. Kozak, A. A. Andales, L. Ma

Abstract. *A recent study showed that the pore-size distribution index (λ) of the Brooks-Corey equation related and scaled cumulative infiltration (I) across eleven textural classes under different rainfall and initial conditions using normalization of the Green-Ampt equation or implicit empirical relations. The initial objectives herein were to (1) explore if more explicit, easy to use, and compact scaling could be achieved through relationships between the parameters of the empirical Lewis-Kostiakov (L-K) infiltration equation (I = cumulative infiltration = kt^{α}; t = time; α, k = constants) and λ or the effective saturated hydraulic conductivity ($\overline{K}_s$) across eleven soil types for instantaneous incipient (zero-head) ponding cases; and (2) in the process, look for a more physical interpretation of the parameters and their dependence on initial soil water content. The Green-Ampt infiltration method in the Root Zone Water Quality Model (RZWQM) was used to generate simulated values for instantaneous zero-head infiltration at two initial pressure heads (–1500 and –100 kPa) in eleven homogeneous textural-class mean soils for 5 h, using the detailed Brooks-Corey hydraulic parameters for each soil. The two L-K parameters (α, k) were shown to have fairly strong explicit relationships with λ (r^2 = 0.78 to 0.88) and stronger relationships with $\overline{K}_s$ (r^2 = 0.94 to 0.99) across the eleven textural classes. Additionally, α was essentially the same for the two initial pressure heads, and its value varied from 0.5 for clay soil to 0.58 for sand, indicating the dominance of sorptivity for clay and the increasing gravity effect for lighter textures, as expected from the theory. The intercept k varied with the pressure head condition but was related to the initial soil water deficit in the same way as sorptivity. Upper time limits for the L-K equation (t_b) to be applicable were also more strongly related to $\overline{K}_s$ (r^2 = 0.99) in all soils. A larger-time (beyond t_b) extension of the L-K equation proposed in the literature was also shown to be valid, thus making it more valuable. The L-K equation was then extended to non-instantaneous ponding infiltration for several rainfall intensities ($I - I_p = k'(t - t_p)^{\alpha'}$; I_p = I at incipient ponding time t_p). The new parameters α′ and k′ for each rainfall intensity were again found to be strongly related to $\overline{K}_s$ or λ, and their variation with respect to initial pressure head was similar to that of α and k. This study provides a simple new method to quickly estimate the variation of infiltration with soil type on a landscape, scale up infiltration from small to large areas, and estimate effective average parameters for modeling large areas. The study also establishes a more physical basis for the L-K equation parameters and shows that it can be extended to large times and to infiltration of rainfalls, just like the Green-Ampt equation.*

Keywords. *Green-Ampt equation, Hydrological modeling, Incipient ponding infiltration, Initial soil moisture on infiltration, Non-instantaneous ponding infiltration, Physical basis of Kostiakov equation parameters, Root Zone Water Quality Model, RZWQM.*

Scaling has been used as a simple method to approximately describe field spatial variability of soil hydraulic properties (Pachepsky et al., 2003; Nielsen et al., 1998; Warrick et al., 1977; Simmons et al., 1979; Russo and Bresler, 1980), as well as characteristics derived from these, such as infiltration, drainage, and available water (Sharma et al., 1980; Simmons et al., 1979). The measured volume curves for each of these properties from many experimental sites and different depths are related to a representative mean curve by choosing a single factor for each site and depth.

As summarized by Tillotson and Nielsen (1984), there are essentially two methods to derive the scaling factors: (1) the dimensional analysis technique, which is based on the existence of physical similarity in the system (e.g., Miller and Miller, 1956); and (2) the empirical method, called function normalization, which is based on regression analysis (e.g., Warrick et al., 1977). The similar-media scaling of Miller and Miller (1956) and the fractal-based approaches of Tyler and Wheatcraft (1990), Rieu and Sposito (1991), and Hunt and Gee (2002a, 2002b) are examples of the first method. Most of the scaling work cited above has extended the similar-media scaling concept to field soils that are generally "non-similar" by invoking additional empirical assumptions

Submitted for review in July 2004 as manuscript number SW 6575; approved for publication by the Soil & Water Division of ASABE in August 2007.

The authors are **Lajpat R. Ahuja,** Soil Scientist and Research Leader, USDA-ARS Agricultural Systems Research Unit, Fort Collins, Colorado; **Joseph A. Kozak,** Research Scientist, Metropolitan Water Reclamation District of Greater Chicago, Cicero, Illinois; **Allan A. Andales, ASABE Member Engineer,** Assistant Professor of Irrigation and Water Science, Department of Soil and Crop Sciences, Colorado State University, Fort Collins, Colorado; and **Liwang Ma,** Soil Scientist, USDA-ARS Agricultural Systems Research Unit, Fort Collins, Colorado. **Corresponding author:** Lajpat R. Ahuja, USDA-ARS Agricultural Systems Research Unit, 2150 Centre Ave., Building D, Suite 200, Fort Collins, CO 80526; phone: 970-492-7315; fax: 970-492-7310; e-mail: Laj.Ahuja@ars.usda.gov.

and using a regression method. This approach has been very useful for describing spatial variability, watershed modeling, and estimation of hydraulic properties. In this study, we pursue the empirical scaling method.

Some recent studies have demonstrated empirical scaling across widely dissimilar soil texture classes from sands to clay. Williams and Ahuja (2003) showed that the textural class-based soil water retention curves (water content-matric potential relationships below the air-entry values), obtained from using the geometric-mean Brooks and Corey (1964) parameters for eleven soil textural classes of Rawls et al. (1982), could be scaled using their log-log slope, that is, the pore-size distribution index (λ, unitless), as the single scaling parameter. Assouline (2005) also described relationships of λ with characteristics of hydraulic functions. In more recent work, Kozak and Ahuja (2005) found that the air-entry pressure head (ψ_b, L) and the saturated hydraulic conductivity ($\overline{K}_s$, L T^{-1}) of the above textural class mean soils were also strongly correlated to λ. The air-entry value also determines the saturated soil water content (θ_s), as once the air-entry value is set on the log($\theta - \theta_r$) versus log λ curve (where θ and θ_r are the current and residual volumetric water contents, respectively), the ($\theta_s - \theta_r$) is also fixed (where θ_s is the saturated volumetric water content). Thus, the λ values, with θ_r for a textural class assumed to be known, could practically determine both the basic soil hydraulic relationships of water retention and conductivity. Kozak and Ahuja (2005) then found that infiltration across soil textural classes could be scaled by λ using the normalized Green-Ampt infiltration equation (Green and Ampt, 1911). They also found strong implicit, empirical relationships of infiltration and soil water content changes during subsequent redistribution among the eleven textural classes as a function of their λ values. Cumulative infiltration (*I*) and the average profile soil water contents after infiltration for fixed times could be expressed as log-log linear functions of λ, e.g., log $I = a + b(\log \lambda)$. The coefficients *a* and *b* were empirical functions of rainfall intensities, initial conditions, and time.

This study was primarily aimed at exploring a more explicit, easier to use, and compact scaling approach for infiltration. We wanted to investigate whether the parameters of an established explicit infiltration-time equation could be expressed as functions of λ or $\overline{K}_s$, initially for the basic case of instantaneously incipient-ponded (zero pressure head at the soil surface) water infiltration, across the eleven textural classes. For this purpose, the following empirical, two-parameter equation of cumulative infiltration, used in the literature, appeared to be most suitable to use:

$$I = kt^{\alpha} \tag{1}$$

where *I* is the cumulative infiltration (L), *t* is time (T), and *k* and α are empirical coefficients (L $T^{-1/2}$ and unitless, respectively). This equation applies only for early to intermediate infiltration times before gravity begins to dominate and the infiltration rate approaches a constant value. This equation has been most commonly called the Kostiakov equation (Kostiakov, 1932). However, Swartzendruber (1993) has made a strong case that this equation should be attributed to Lewis (1937) as well. This Lewis-Kostiakov (L-K) equation is mathematically convenient. It expresses infiltration volume explicitly as a function of time, and coefficients can be found by straight-line fit of infiltration depth *I* versus time on a log-log plot. Original developers and some other investigators used it for infiltration and runoff prediction (Lewis, 1937; Swartzendruber and Huberty, 1958). Because of its simplicity and ease of use, this equation is very commonly used in agricultural engineering for designing surface irrigation and estimating infiltration in level borders and furrows (Walker and Skogerboe, 1987; Clemmens et al., 2001; Colla et al., 2000; Bautista et al., 2001; Cavero et al., 2001; Oyonarte and Mateos, 2002). The equation is prescribed as a standard for evaluation of surface irrigation by ASABE (*ASABE Standards*, 2003; also see NRCS, 1997, 2005). Obviously, the equation is considered adequate for most common irrigation durations.

Equation 1 has been slightly modified by various investigators to improve its fit for certain conditions (Bautista et al., 2001). In particular, to extend its applicability for long times, Clemmens (1981) proposed the following step functions:

$$I = kt^{\alpha}; \quad t \le t_b \tag{2}$$

$$I = kt_b^{\alpha} + \overline{K}_s(t - t_b); \quad t > t_b \tag{3}$$

Equating the slopes *dI*/*dt* (infiltration rate) of equations 2 and 3 at time t_b gives:

$$t_b = \left(\frac{\alpha k}{\overline{K}_s} \right)^{\frac{1}{1-\alpha}} \tag{4}$$

where t_b (T) is the time up to which equation 2 holds, and $\overline{K}_s$ (L T^{-1}) is the effective saturated hydraulic conductivity of the wetted profile used in generating the simulated data. The determination of t_b by equation 4 may extend the range of applicability of equation 2. The above extension of the L-K equation does not add any new empirical coefficient, and the coefficients to be determined remain *k* and α.

If we can show that all the three parameters of the L-K infiltration equations (eqs. 2 and 3) for different soil types are related to just one parameter λ (or $\overline{K}_s$) of the respective soil type, this will be a valuable contribution to new knowledge of how infiltration on different soils is explicitly related. The relationships will allow researchers to quickly estimate all three parameters of these equations and hence the infiltration distribution on a landscape due to variation in soil type. This distribution can then be used to estimate effective average parameters for modeling a large variable area and scale up infiltration from individual soils to large fields and sub–watersheds. A scientifically robust scaling framework is the greatest need for making breakthroughs in transferring research across scales and understanding and managing large areas (National Research Council, 1991). In the process of exploring scaling of parameters across soil textural classes, it would be very useful to look for a more physical interpretation of the L-K parameters and their dependence on initial soil water content.

It would also be very useful if we could extend the above functional analysis to infiltration of rainfalls where the incipient ponding or surface saturation is not instantaneous and occurs after a certain time that depends upon rainfall intensity and soil type. To explore this possibility, we hypothesized the following empirical two-parameter equations of water infiltration after incipient ponding:

$$I - I_p = k'(t - t_p)^{\alpha'}; (t - t_p) \le (t_b' - t_p) \quad (5)$$

where t_p is the time to incipient ponding for a given soil and rainfall intensity, I_p is the cumulative infiltration until t_p, and k', α', and t'_b are new constants. Equation 5 embodies an additional assumption that the process of infiltration after incipient ponding becomes similar to that of instantaneous ponding. Such an assumption has been used often for the Green-Ampt model of infiltration after ponding (Mein and Larson, 1973; Hachum and Alfaro, 1977; Wilson et al., 1982).

The I_p for any given soil and rainfall intensity can be estimated from the equation based on the Green-Ampt approach (Kozak and Ahuja, 2005):

$$I_p = \frac{G(\theta_s - \theta_i)\overline{K}_s}{(r - \overline{K}_s)} \quad (6)$$

where G is the wetting front suction, $\overline{K}_s$ is the effective saturated hydraulic conductivity, r is the rainfall intensity, θ_s is the effective saturated soil water content, and θ_i is the initial soil water content. The wetting front suction (G) is a function of λ and an air entry pressure head ψ_b (Smith, 2002), but may be expressed as a function of just λ or $\overline{K}_s$ based on relations between ψ_b and λ and $\overline{K}_s$ and λ (Kozak and Ahuja, 2005).Thus, for any given rainfall intensity r and soil type of known $\overline{K}_s$ or λ (Kozak and Ahuja, 2005), I_p can be derived from equation 6. The unsaturated hydraulic conductivity corresponding to θ_i is assumed negligible in deriving equation 6.

The main objectives of this study were to (1) investigate for the purpose of scaling the applicability of the water infiltration L-K equation (eq. 2), subject to the basic case of zero pressure head at the soil surface, across soil textural classes, and the relationships of its parameters (α and k) to the textural class mean λ or $\overline{K}_s$ values; (2) in the process, look for a more physical interpretation of the parameters α and k, and their dependence upon the initial soil water content; and (3) to investigate the relationship, if any, of t_b to the textural class mean λ or $\overline{K}_s$ values. A challenge to the use of equation 2 at the field scale is that its parameters lump the effects of soil heterogeneities, pressure versus gravity gradients, and initial soil water contents. These objectives should help resolve some of these issues and hopefully provide a more physical interpretation of the parameters of equation 2.

An additional purpose of the study was to investigate the applicability and scaling relationships for the parameters of the extended L-K equation (eq. 5) for non-instantaneous ponding conditions (rainfall infiltration) with respect to each of the above objectives.

Materials and Methods

The data needed for investigations of the objectives were generated theoretically using the Green-Ampt (Green and Ampt, 1911) equation as implemented in the Root Zone Water Quality Model (RZWQM; Ahuja et al., 2000). The Green-Ampt (G-A) equation can be derived from a simplification of the Richards equation (Morel-Seytoux and Khanji, 1974; Ahuja, 1983). It has been proven reasonably accurate in predicting infiltration in comparison with the solutions of the Richards equation and measured data under many conditions (Bouwer, 1969; Childs and Bybordi, 1969; Mein and Larson, 1973; Idike et al., 1980; Hachum and Alfaro, 1977; Rao et al., 2006). Therefore, our use of the infiltration values generated by employing the Green-Ampt equation for the purpose of this study, evaluating equations 2, 3, and 5 and the relationships of their parameters across soil textural classes, is justified. The main limitation of the Green-Ampt model is thought to be the assumption of an abrupt wetting profile during infiltration; it is actually the requirement that the progressive wetting profiles have a similarity in shape (Morel-Seytoux and Khanji, 1974; Ahuja, 1983). The effect of this assumption on the calculation of infiltration rates is small, if any. The Brooks and Corey (1964) soil hydraulic parameters for all soils used in the simulations were geometric mean values of a large number of measured data for each textural class (Rawls et al., 1982). This application is a good use of the established theory with measured inputs to develop simpler empirical relations for practical purposes, rather than undertaking laborious and time-consuming experimental measurements of infiltration and soil hydraulic properties of numerous soil types and several precipitation intensities. The data variability will likely be so great that meaningful relations could not be identified. The theory-based results will be verified against experimental data in future studies. Several cases of incipient ponding and non-instantaneous ponding (e.g. lower intensity rainfall) were examined.

Incipient Ponding

Theoretical studies to generate infiltration under incipient ponding (instantaneous zero pressure head at the soil surface) were performed using the RZWQM in eleven textural class mean soils (Rawls et al., 1982; Kozak and Ahuja, 2005). RZWQM is designed for rainfall infiltration that includes two surface boundary conditions: initially the influx rate equal to the rainfall rate until the soil surface gets saturated (zero pressure head), and the constant zero pressure head thereafter. In order to obtain nearly instantaneous incipient ponding, very high rainfall intensities (100 to 500 cm h^{-1}) were employed for all soils. The rainfall intensities varied with soil type, with sandy soil requiring the highest intensity to achieve nearly instantaneous incipient ponding. Upon a precipitation event in RZWQM, the method of Green and Ampt with the wetting front pressure head obtained from integration of the soil relative unsaturated hydraulic conductivity curve between initial and surface pressure heads (Ahuja et al., 2000) is used to predict the infiltration rates and cumulative infiltration in the soil profile (Ahuja et al., 1993, 2000). The effective saturated $\overline{K}_s$ is set to K_s/2.0 to account for entrapped air and viscous resistance effects on saturated conductivity; the number 2.0 is the viscous resistance correction factor (Morel-Seytoux and Khanji, 1974; Ahuja et al., 2000). Under the high rainfall intensities used here, incipient surface ponding was essentially instantaneous. The lower boundary condition for the deep soil profiles used in this study was a unit hydraulic gradient, i.e., free gravity flow.

Eleven homogeneous soil profiles (300 cm deep) with hydraulic properties corresponding to the measured geometric mean properties of eleven soil textural classes ranging from sand to clay, were the subject of this infiltration study. The measured textural class mean properties along with the hydraulic parameters of each soil used in simulations are summarized in table 1 (Rawls et al., 1982). The soil profiles were

Table 1. Hydrological properties of eleven textural classes (Rawls et al., 1982).

Texture	Mean Total Porosity, θ_s ($cm^3\ cm^{-3}$)	Geometric Mean Bubbling Pressure, $\lvert\psi_b\rvert$ (kPa)	Mean Residual Saturation, θ_r ($cm^3\ cm^{-3}$)	Geometric Mean Pore Size Distribution index, λ	Mean Saturated Hydraulic Conductivity ($cm\ h^{-1}$)
Sand	0.437	0.726	0.02	0.591	21.00
Loamy sand	0.437	0.869	0.035	0.474	6.11
Sandy loam	0.453	1.466	0.041	0.322	2.59
Loam	0.463	1.115	0.027	0.22	1.32
Silt loam	0.501	2.076	0.015	0.211	0.68
Sandy clay loam	0.398	2.808	0.068	0.25	0.43
Clay loam	0.464	2.589	0.075	0.194	0.23
Silty clay loam	0.471	3.256	0.04	0.151	0.15
Sandy clay loam	0.430	2.917	0.109	0.168	0.12
Silty clay loam	0.479	3.419	0.056	0.127	0.09
Clay	0.475	3.73	0.09	0.131	0.06

subjected to 5 h infiltration events at two initial soil water pressure head conditions of –1500 and –100 kPa; these pressure heads represent a good practical range of antecedent water contents encountered in the field. For each soil type and initial condition, equation 2 was first fitted to the G-A infiltration simulation results to derive the L-K parameters, and then these fitted parameters α, k, and t_b were related with the Brooks and Corey λ or $\overline{K}_s$.

Non-Instantaneous Ponding

Theoretical studies to generate infiltration under varying rainfall intensities were also performed using the RZWQM for the same eleven textural class soils (table 1) given in the previous section. The effective saturated hydraulic conductivity $\overline{K}_s$ was, again, set to $K_s/2.0$. The upper boundary condition during infiltration was the constant influx equal to the rainfall rate until the incipient ponding time, and a constant zero pressure head thereafter. The lower boundary condition for the deep soil profiles used was a unit hydraulic gradient, i.e., free gravity flow.

The soil profiles were subjected to 5 h precipitation events for each of the rainfall intensities of 20, 10, 5, and 2.5 cm h^{-1} at two initial soil pressure heads of –1500 and –100 kPa (table 2). All infiltration events where incipient ponding at the soil surface was not instantaneous were the primary subject of this study. However, some results obtained for higher rainfall intensities applied to induce instantaneous incipient ponding (500 cm h^{-1} for sand and 100 cm h^{-1} for all other soils) were also used as limits. The I and t from RZWQM simulations for all scenarios were analyzed, and ponding was assumed to occur once the infiltration rate fell below the rainfall rate. For each soil type and initial condition, the infiltration simulation results based on the Green-Ampt approach were used to evaluate the fit of equation 5 and the relationship of the parameters α', and k' with the Brooks and Corey λ or $\overline{K}_s$. Within the 5 h infiltration events, the time t_b' was not reached in all cases studied.

Table 2. RZWQM simulation scenarios for rainfall infiltration in the eleven textural class mean soils.

Scenario	Rainfall Intensity ($cm\ h^{-1}$)	Duration of Rain Event (h)	Initial Soil Water Pressure Head (kPa)
1	20	5	–1500
2	10	5	–1500
3	5	5	–1500
4	2.5	5	–1500
5	20	5	–100
6	10	5	–100
7	5	5	–100
8	2.5	5	–100

Results and Discussion

Incipient Ponding

Figures 1a and 1b show the log-log plot of I vs. t for selected soils (sand, loamy sand, loam, and clay) for the two initial pressure heads (–1500 and –100 kPa), respectively. All logs referred to herein are $\log_{10}$. For sand and loamy sand, curvilinear plots resulted over 5 h of the infiltration event. For these soils, the plotted values were divided into two segments according to equations 2 and 3. The time t_b, when the values started to deviate from a linear relation, was determined as follows: a line was fitted to the values, and equation 2 was considered applicable up to the point where r^2 values started to fall below 0.998. This r^2 was used (albeit, arbitrarily but reasonably) as it represents a high correlation and visually matched up to the inflection in the curves. Some deviation from the regression lines occurred, but this may be at least partly due to minor numerical simulation errors. The α and log k values from equation 2 were then derived from regression to these values (table 3), and equation 4 was used to determine t_b. Thus, when $t < t_b$, a very strong linear relationship was observed between I and t for all four soils, i.e., $r^2 \geq 0.998$. Table 3 summarizes the α and log k values for all soils, along with their expected t_b values calculated from equation 4. Only for sand and loamy sand soils, the t_b values fell within the 5 h duration of the simulated infiltration data used in this study. The t_b values for sand and loamy sand in figures 1a and 1b are very close to calculated values given in table 3.

The α and log k values at the –1500 kPa initial pressure head are plotted versus λ in figures 2a and 2b, respectively. Although fairly high r^2 values were observed between α and λ (fig. 2a) and log k and λ (fig. 2b) (r^2 values of 0.80 and 0.88, respectively), there was a good amount of scatter in the relationships, particularly between α and λ. There is an apparent discontinuity at $\lambda = 0.22$ (fig. 2a) that may suggest two linear equations to fit the data. Relationships were greatly improved when plotting α and log k versus the log of the effective saturated hydraulic conductivity ($\overline{K}_s$) for each soil (fig. 3); the r^2 values for α and log k were 0.95 and 0.99, respectively. It is interesting to observe that α and log k had a linear relationship with λ, but a logarithmic relationship with $\overline{K}_s$.

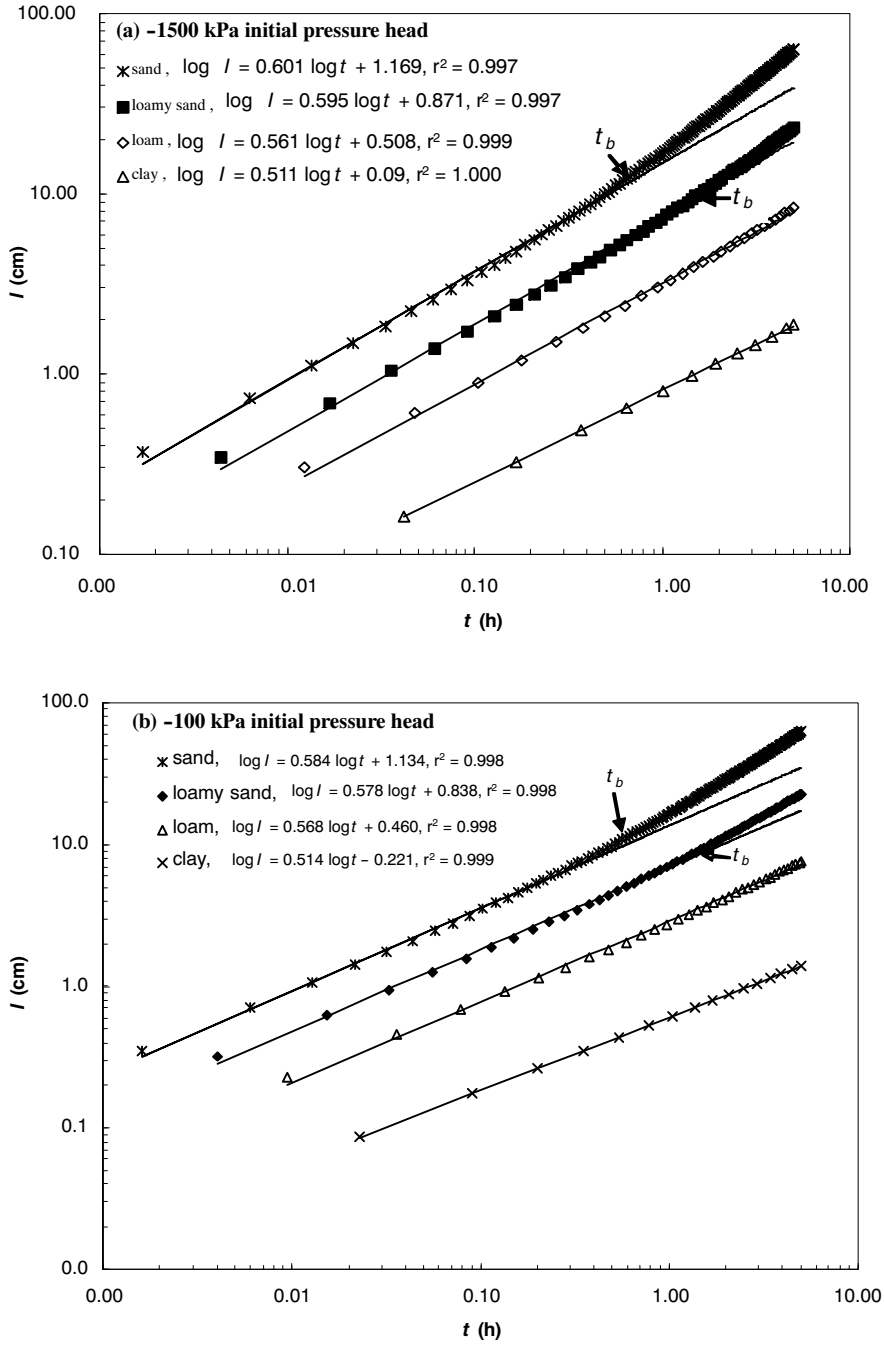

Figure 1. (a) Log-log relationship between cumulative infiltration *I* (cm) and time *t* (h) for four of the eleven textural classes at an initial pressure head of -1500 kPa, and (b) log-log relationship between *I* and *t* for four of the eleven textural classes at an initial pressure head of -100 kPa. The last value of *t* is 5.0 h. For sand and loamy sand soils, the lines fitted to values for $t < t_b$ are extrapolated in both cases. The t_b values shown in the figures were calculated by equation 4, as given in table 3. These values are 0.62 and 1.43 at -1500 kPa and 0.72 and 1.51 at -100 kPa for sand and loamy sand soils, respectively.

The relationships of α and log *k* values for -100 kPa initial pressure head with λ were very similar to those in figure 2a, with r^2 equal to 0.76 and 0.88, respectively. As before, the relationships of α and *k* with $\overline{K}_s$ were stronger, with r^2 equal to 0.94 and 0.99, respectively. Thus, for both initial pressure heads, the Lewis-Kostiakov parameters versus log $\overline{K}_s$ yield better r^2 results and acceptable relationships.

Table 3 indicates that the α values were approximately equal for the two initial pressure heads. It was also observed that the α values for clay soil at both initial pressure heads were close to 0.5, but gradually increased for other textural classes, to 0.58 for loamy sand and sand. The slope of 0.5 is expected in early stages when gravity is negligible (Philip, 1957):

$$I = St^{1/2} \quad (7)$$

where *S* ($L\,T^{-1/2}$) is sorptivity. The increase in the slope α for sandier soils indicates that gravity has started to contribute to infiltration rate in these soils.

Table 3. Kostiakov parameters from equation 2 across soil textural classes for the case of instantaneous incipient ponding.

	α		log *k*		t_b (h)	
Texture	−1500 kPa	−100 kPa	−1500 kPa	−100 kPa	−1500 kPa	−100 kPa
Sand	0.5839	0.5839	1.1434	1.1601	0.62	0.72
Loamy sand	0.5783	0.5783	0.8550	0.8380	1.43	1.51
Sandy loam	0.5679	0.5678	0.7331	0.6933	6.14	5.50
Loam	0.5607	0.5680	0.5080	0.4598	25.77	19.60
Silt loam	0.5322	0.5377	0.4709	0.4031	30.16	22.54
Sandy clay loam	0.5268	0.5306	0.3483	0.2776	15.93	12.80
Clay loam	0.5212	0.5247	0.2004	0.1158	41.37	29.83
Silty clay loam	0.5159	0.5194	0.1422	0.0350	106.25	68.83
Sandy clay	0.5169	0.5208	0.0152	−0.0896	71.11	48.21
Silty clay	0.5135	0.5164	0.0063	−0.1175	203.84	122.63
Clay	0.5112	0.5140	−0.0904	−0.2206	181.38	110.58

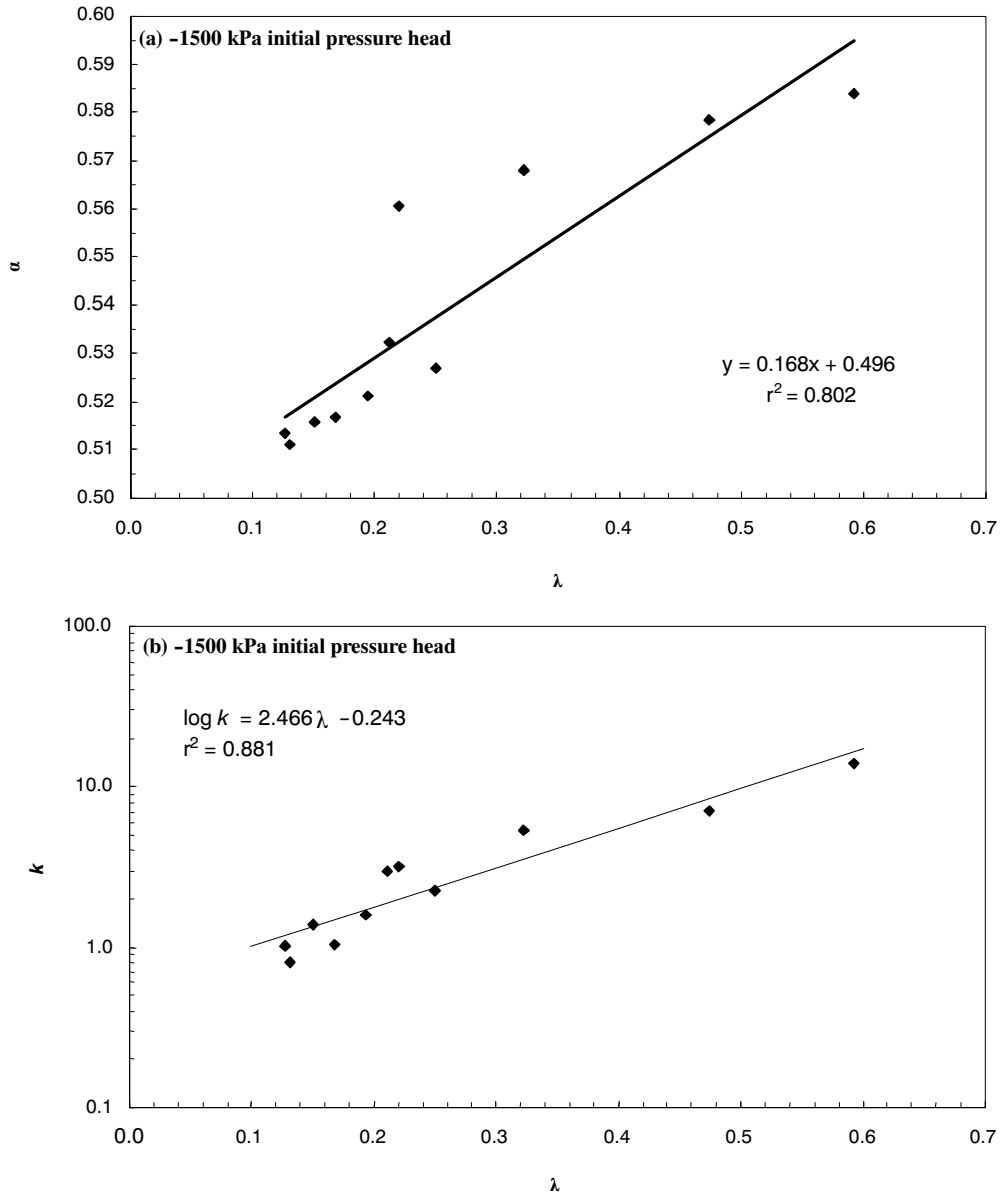

Figure 2. Relationship between the Lewis-Kostiakov equation parameters (a) α and (b) *k* and the pore-size distribution index λ for the eleven textural classes at an initial pressure head of −1500 kPa.

On the other hand, the log *k* values shown in table 3 varied with initial pressure head, especially with respect to the heavier soils. According to equation 7, in early stages, intercept *k* of equation 2 should be the same as *S*. Based on the Green-Ampt infiltration model, *S*, and hence *k* at early stages, can be obtained from (Smith, 2002; pg. 76):

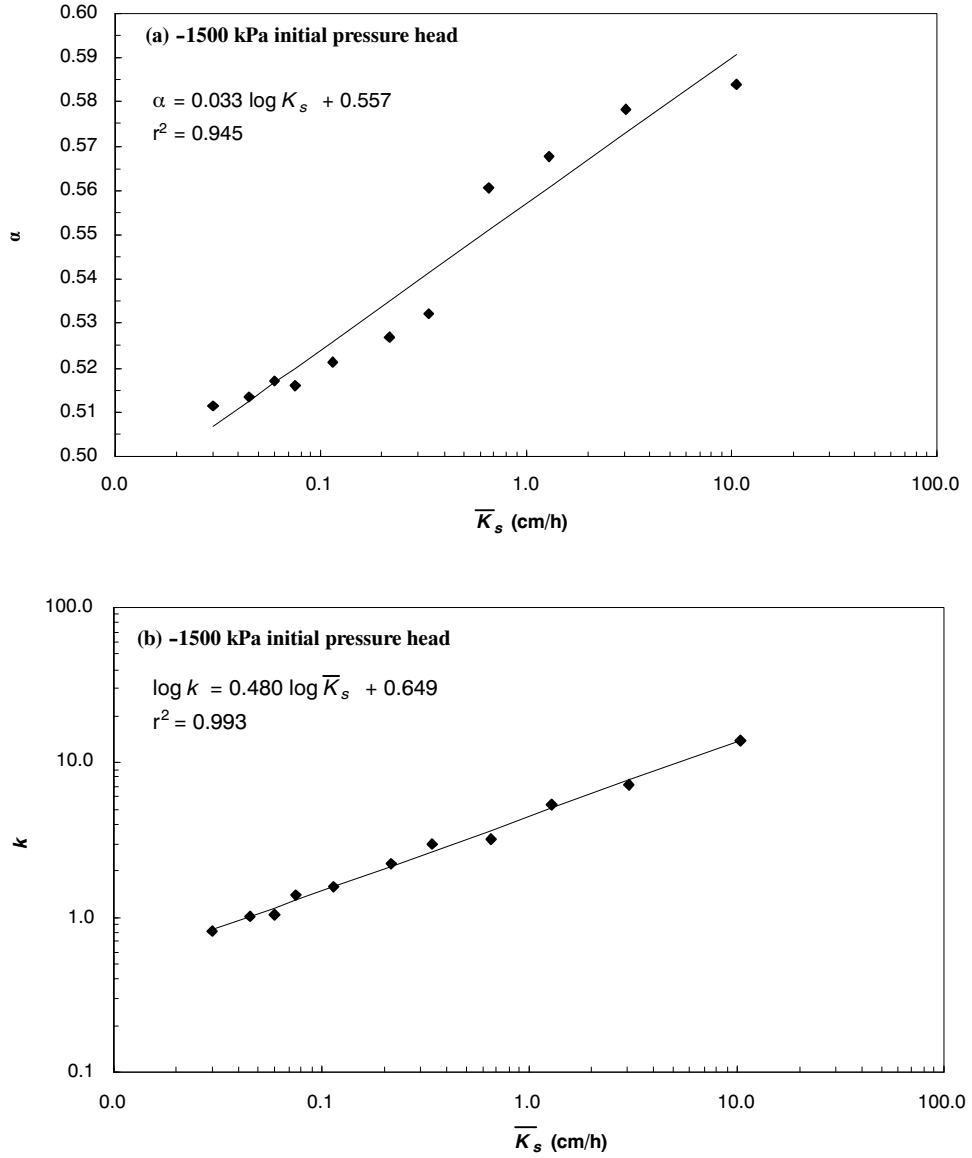

Figure 3. Relationship of parameters (a) a and (b) *k* with soil saturated hydraulic conductivity $\overline{K}_s$ for the eleven textural classes at an initial pressure head of -1500 kPa.

$$k \approx S = \sqrt{\frac{G(\theta_s - \theta_i)(K_s - K_i)}{2}} \tag{8}$$

where θ_i ($L^3\ L^{-3}$) is the initial soil water content corresponding to initial pressure head (-1500 or -100 kPa) calculated from the Brooks-Corey water retention relation, θ_s ($L^3\ L^{-3}$) is the saturated soil water content, K_i ($L\ T^{-1}$) is the hydraulic conductivity at $\theta = \theta_i$, and G ($L\ T^{-1}$) is given as:

$$G = \frac{2 + 3\lambda}{1 + 3\lambda}\psi_b \tag{9}$$

where ψ_b is the air-entry pressure head. If θ_i values are small, so that K_i at $\theta = \theta_i$ can be assumed to be negligible ($K_i = 0$) and G can be assumed constant at two different initial θ_i values (i.e., two different pressure heads), then the k values at the two pressure heads may be related as:

$$\frac{k_{h2}}{k_{h1}} = \sqrt{\frac{(\theta_s - \theta_i)_{h1}}{(\theta_s - \theta_i)_{h2}}} \tag{10}$$

where $h1$ is pressure head 1, and $h2$ is pressure head 2.

Equation 10 was applied to predict log k at -100 kPa for all soils from the -1500 kPa results of log k. Figure 4 shows this predicted log k at -100 kPa versus the log k obtained from fitting to the Green-Ampt simulation results at -100 kPa. Very good agreement is observed between the Green-Ampt derived and predicted log k across all soils (RMSE = 0.006 cm). Thus, equation 10 can approximately describe the dependence of k on initial pressure head, from essentially dry to moist soil conditions (-1500 to -100 kPa). With α remaining essentially the same, the effect of initial conditions on both parameters of equation 2 is accounted for.

Finally, using the parameters α and k derived from equation 2, equation 4 was applied to determine t_b for the step

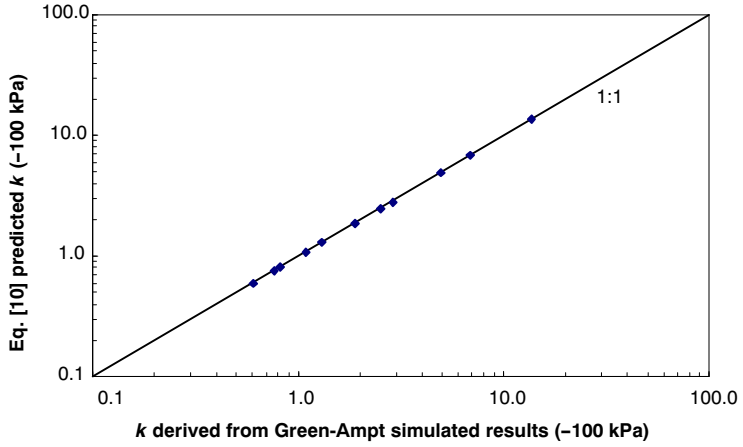

Figure 4. Comparison of equation 10 predicted *k* and Green-Ampt derived *k*. The square symbols are for eleven different textural classes, and *k* increases with coarseness of texture (table 3).

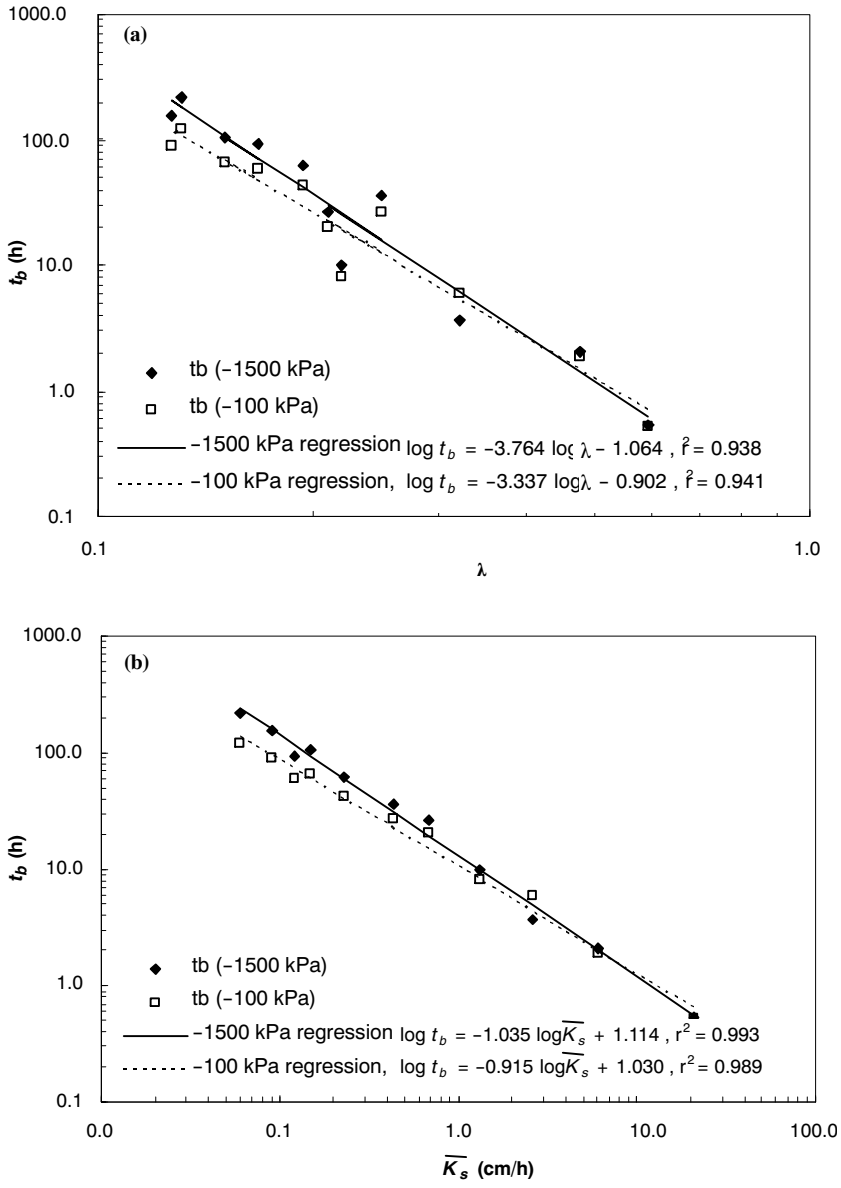

Figure 5. (a) Log-log relationship between time (t_b) of equation 4 and λ for the eleven textural classes at the two initial pressure heads, and (b) log-log relationship between t_b and $\overline{K_s}$ for the eleven textural classes at the two initial pressure heads.

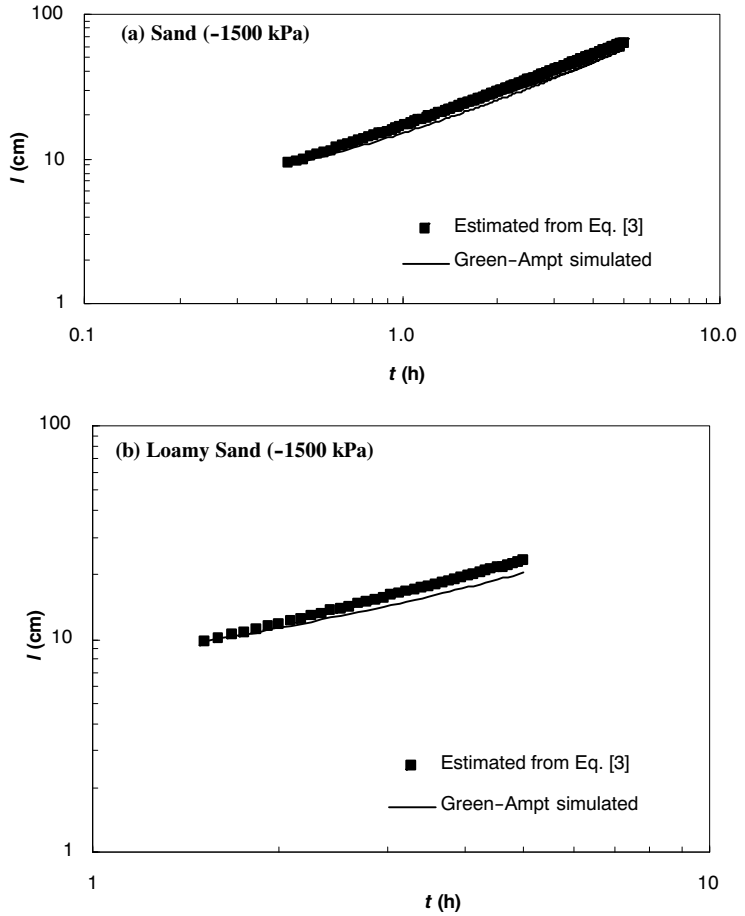

Figure 6. (a) Log-log relationship between *I* and *t* for sand at large times > t_b, beyond the range of applicability of the Lewis-Kostiakov equation, at the initial pressure head of -1500 kPa, for original Green-Ampt simulated *I* and *I* estimated from equation 3, and (b) log-log relationship between *I* and *t* for loamy sand at large times > t_b, beyond the range of applicability of the Lewis-Kostiakov equation, at the initial pressure head of -1500 kPa for original Green-Ampt simulated *I* and *I* estimated from equation 3.

functions (eqs. 2 and 3) for all soils (table 3), even though t_b was observed in only two of the soils during the 5 h infiltration (fig. 1). Log-log plots of t_b versus λ and $\overline{K}_s$ for both pressure heads are shown in figures 5a and 5b, respectively. Strong linear relationships are observed between t_b and λ as well as t_b and $\overline{K}_s$ for both initial pressure heads. The relationships with $\overline{K}_s$ are stronger. The relationships for the two initial pressure heads are slightly different but close. Validity of the calculated t_b values was tested for sand and loamy sand soils, which exhibited a curvilinear trend in the results (figs. 1a and 1b). Equation 3 was used to estimate *I* when $t > t_b$. Figures 6a and 6b show the log-log plots of the RZWQM (G-A) simulated *I* vs. *t* and the predictions based on equation 3 for an initial pressure head of -1500 kPa for the two soils. Very good agreement was observed between simulated and predicted *I* (RMSE = 0.042 and 0.049 cm for sand and loamy sand, respectively). Similar agreement was observed between simulated and predicted *I* in sand and loamy sand for an initial pressure head of -100 kPa (RMSE = 0.056 and 0.059 cm, respectively).

The above results show that the parameters of the Lewis-Kostiakov equation (eq. 2) for instantaneous zero-head ponded conditions are related to λ or $\overline{K}_s$, more strongly to $\overline{K}_s$, across the eleven mean textural class soils. It is further shown that the effect of initial soil water content on the parameters can be estimated. The limiting time t_b can also be approximately calculated. This study thus gives empirical relations for parameters of the Lewis-Kostiakov equation with soil properties (λ or $\overline{K}_s$) and initial conditions, and permits easy extension of the infiltration equation from one soil type to another, even beyond time t_b, the time limit of applicability of equation 2.

Non-Instantaneous Ponding

It should be made clear upfront that this section deals only with cases where the incipient ponding at the soil surface was not instantaneous. At higher rainfall intensities in this study, some of the soil types did undergo near instantaneous incipient ponding. On the other hand, at low rainfall intensities, some of the soils did not attain incipient ponding at all during the 5 h duration of the infiltration events. In both cases, the data for such soils are not included in the analysis.

Figure 7a shows the log-log plot of $(I - I_p)$ vs. $(t - t_p)$ for the middle loam textural class, for the four rainfall rates at an initial pressure head of -1500 kPa. The data for the 10 and 20 cm h^{-1} rainfall intensities overlapped. Figure 7b shows a similar plot for the sandy loam texture class for the four rainfall rates at an initial pressure head of -100 kPa. The log-log plots of data for each rainfall intensity and soil in figure 7 showed a strong linear relationship, with $r^2 > 0.998$. Much like figure 7, for other soil types, rainfall intensities, and ini-

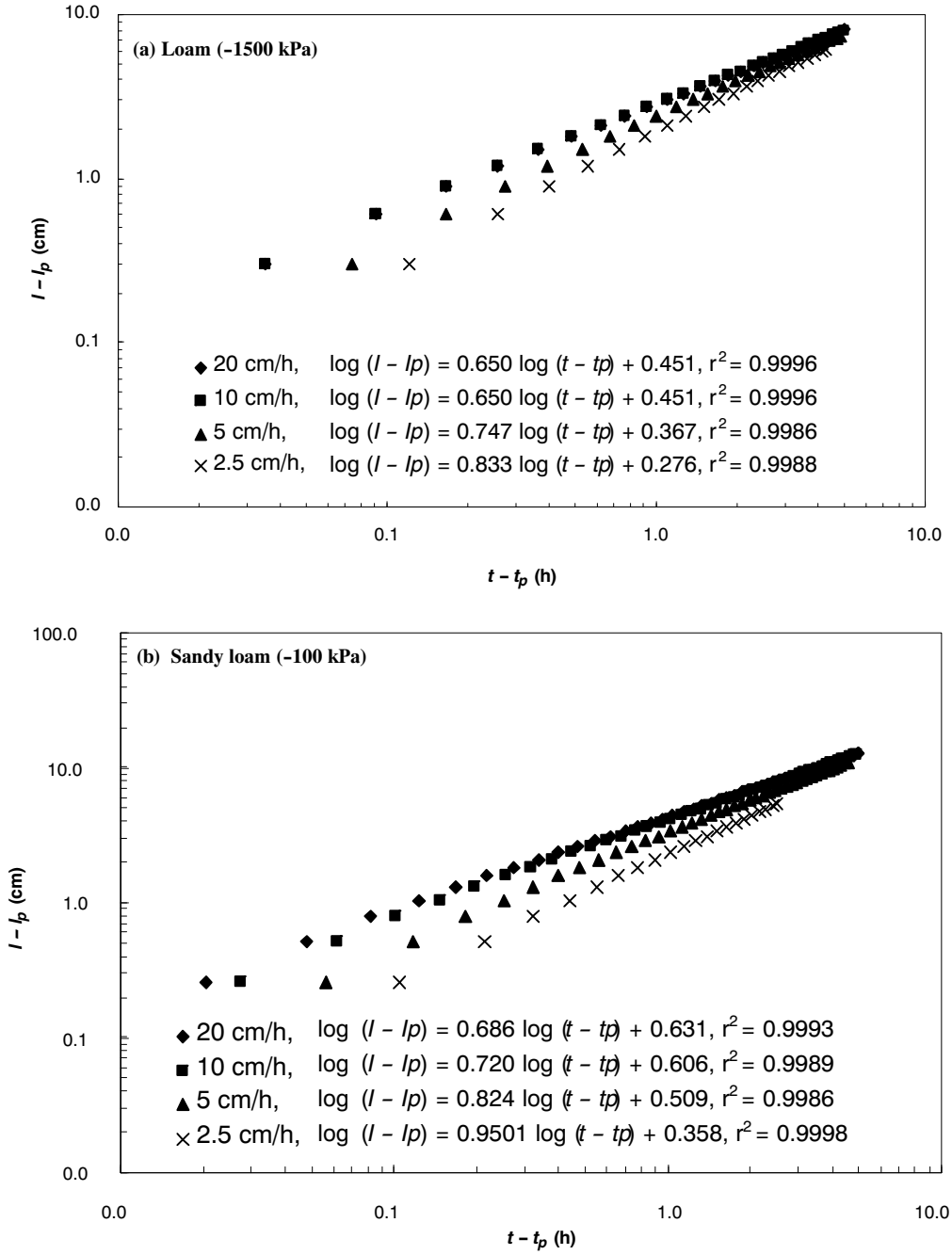

Figure 7. (a) Log-log relationship between cumulative infiltration after ponding ($I - I_p$) and time after ponding ($t - t_p$) for loam at four rainfall intensities and an initial pressure head of -1500 kPa, and (b) log-log relationship between cumulative infiltration after ponding ($I - I_p$) and time after ponding ($t - t_p$) for sandy loam at four rainfall intensities and an initial pressure head of -100 kPa.

tial pressure head conditions, where data were available, the plots showed a very strong linear relationship exhibiting a fit of equation 5 with $r^2 \approx 0.995$ or higher and no upward bend from the line at large times within the 5 h duration. Because of this, no simulation points were excluded from the fit of equation 5. These fits provided α' and k' values for each case, with no t_b' values.

For table 2 scenarios 1 through 4 (rainfall intensities of 2.5 to 20 cm h^{-1} and an initial pressure head of -1500 kPa), linear equations were fitted to the data of α' and log k' values against λ for each rainfall intensity (table 4). The r^2 values for α' versus λ ranged from 0.83 to 0.92. The r^2 values for log k' versus λ ranged from 0.77 to 0.98. The α' and log k' values for each rainfall intensity are plotted versus log $\overline{K}_s$ in figures 8 and 9, respectively. The r^2 values for linear relationship α' versus $\overline{K}_s$ ranged from 0.90 to 0.94. The r^2 values for log k' versus log $\overline{K}_s$ were all close to 0.98. Thus, as in the case of instantaneous ponding, the parameters of equation 5 were more strongly related to log $\overline{K}_s$.

For table 2 scenarios 5 through 8 (rainfall intensities of 2.5 to 20 cm h^{-1} and an initial pressure head of -100 kPa), linear equations of α' and log k' values against λ for each rainfall intensity are given in table 5. The r^2 values for α' versus λ relation ranged from 0.84 to 0.91, and the r^2 values for log k' versus λ ranged from 0.78 to 0.98. Likewise, linear regression

Table 4. Fitted regression lines relating the extended Lewis-Kostiakov equation parameters α′ or k' to the pore-size distribution index λ for the eleven textural classes at an initial pressure head of –1500 kPa and four different rainfall intensities.

	Rainfall Intensity (cm h^{-1})	Regression Equation	r^2
α′ versus λ	2.5	α′ = 1.6672 λ + 0.4032	0.83
	5.0	α′ = 1.018 λ + 0.4673	0.90
	10.0	α′ = 0.7343 λ + 0.4668	0.92
	20.0	α′ = 0.6165 λ + 0.4933	0.90
log k' versus λ	2.5	log k' = 2.703 λ – 0.4514	0.81
	5.0	log k' = 2.1359 λ – 0.2627	0.78
	10.0	log k' = 1.5434 λ + 0.055	0.77
	20.0	log k' = 1.8196 λ + 0.0392	0.98

of α′ and log k' values versus log $\overline{K}_s$ for each rainfall intensity are given in table 6. The r^2 values for α′ versus $\overline{K}_s$ relation ranged from 0.91 to 0.95, and the r^2 values for log k' versus log $\overline{K}_s$ ranged from 0.97 to 0.99. Again, stronger relations are obtained with log $\overline{K}_s$ for this initial pressure head as well.

Overall, the linear relationships between α′ and log k' versus $\overline{K}_s$ were much better than α′ and log k' versus λ. These relationships themselves were, however, also a function of rainfall intensity. Generally, for each soil, as the rainfall intensity decreased, the α′ values increased while the log $k^{'}$ value decreased. The α′ values for each rainfall intensity were essentially the same at both initial pressure heads; however, the $k^{'}$ values differed (see coefficients of regression equations for α′ and log $k^{'}$ in tables 4 and 5).

We further investigated the dependence of $k^{'}$ values on the initial pressure head by predicting log $k^{'}$ at –100 kPa for all soils and all rainfall intensities from the –1500 kPa results of log $k^{'}$ (i.e., using eq. 10). Figure 10 shows the equation 10 predicted $k^{'}$ at –100 kPa versus the $k^{'}$ at –100 kPa derived from Green-Ampt simulations. Good agreement was observed between the Green-Ampt-derived and predicted $k^{'}$ for all soils and rainfall intensities. Thus, equation 10 can approximately describe the dependence of $k^{'}$ on initial pressure head. The initial pressure heads of –1500 and –100 kPa cover a range from dry to moist soil conditions.

Next, we explored empirical functional dependence of the parameters of the fitted relationships between α′ and log $k^{'}$ vs. log $\overline{K}_s$ (figs. 8 and 9; table 6) on rainfall intensity. For this purpose, the fitted relationships in these figures and table 6 were represented as:

$$\alpha' = b + c(\log \overline{K}_s) \qquad (11)$$

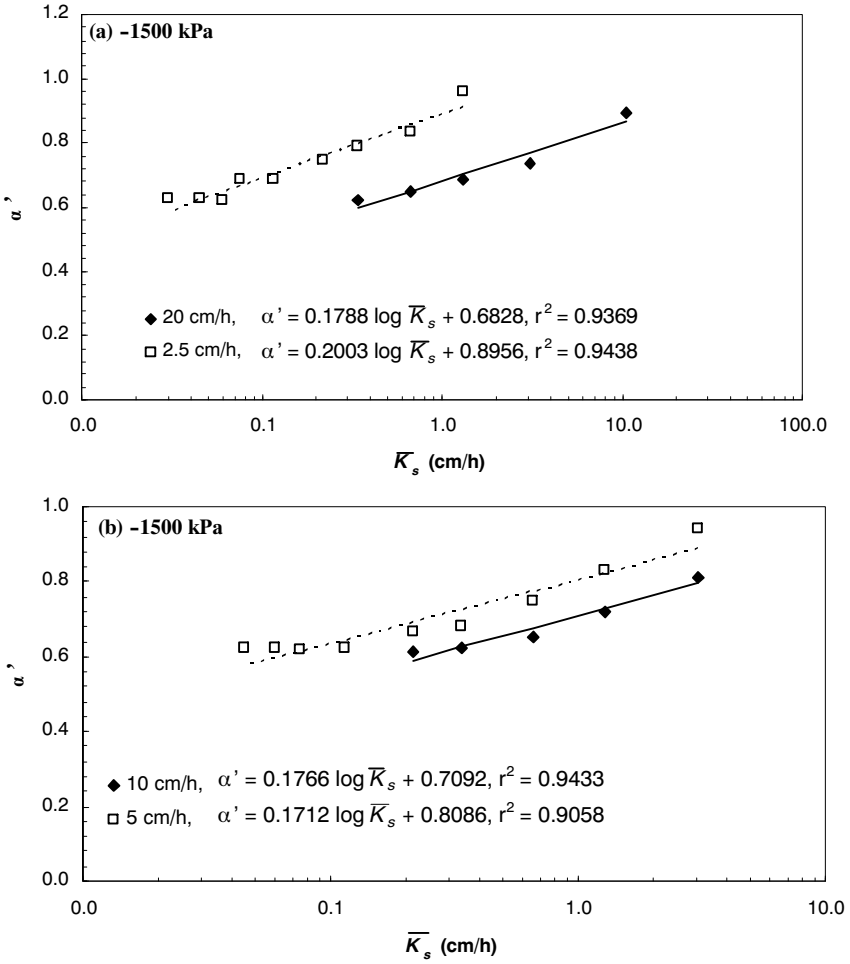

Figure 8. (a) Relationship between the extended Lewis-Kostiakov equation parameter a′ and the saturated hydraulic conductivity $\overline{K}_s$ for the eleven textural classes at an initial pressure head of –1500 kPa and rainfall intensities of 20 and 2.5 cm h^{-1}, and (b) relationship between parameter a′ and the $\overline{K}_s$ for the eleven textural classes at an initial pressure head of –1500 kPa and rainfall intensities of 10 and 5 cm h^{-1}.

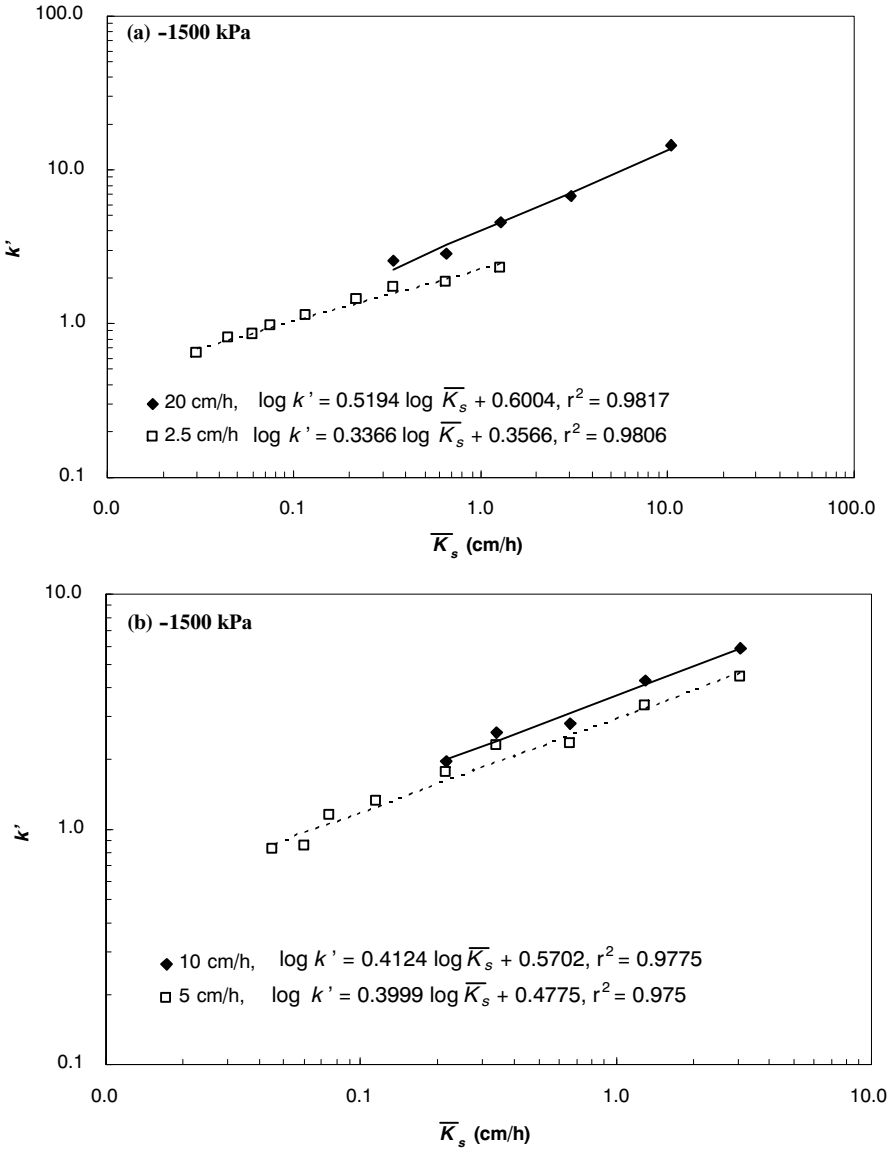

Figure 9. (a) Relationship between the extended Lewis-Kostiakov equation parameter k' and the saturated hydraulic conductivity $\overline{K_s}$ for the eleven textural classes at an initial pressure head of -1500 kPa and rainfall intensities of 20 and 2.5 cm h^{-1}, and (b) relationship between parameter k' and the $\overline{K_s}$ for the eleven textural classes at an initial pressure head of -1500 kPa and rainfall intensities of 10 and 5 cm h^{-1}.

Table 5. Fitted regression lines relating the extended Lewis-Kostiakov equation parameters α' or k' to the pore-size distribution index λ for the eleven textural classes at an initial pressure head of -100 kPa and four different rainfall intensities.

	Rainfall Intensity (cm h^{-1})	Regression Equation	r^2
α' versus λ	2.5	$\alpha' = 1.6687\,\lambda + 0.3911$	0.84
	5.0	$\alpha' = 1.0199\,\lambda + 0.4599$	0.91
	10.0	$\alpha' = 0.7392\,\lambda + 0.4637$	0.91
	20.0	$\alpha' = 0.6215\,\lambda + 0.4913$	0.91
log k' versus λ	2.5	log $k' = 3.2085\,\lambda - 0.6044$	0.81
	5.0	log $k' = 2.4035\,\lambda - 0.3739$	0.79
	10.0	log $k' = 1.731\,\lambda - 0.0399$	0.78
	20.0	log $k' = 1.9527\,\lambda - 0.0377$	0.98

$$\log k' = d + e(\log \overline{K_s}) \quad (12)$$

where b, c, d, and e are empirical coefficients for each rainfall intensity, whose values are given in figures 8 and 9 and table 6. The coefficients were individually plotted as a function of the rainfall intensities r for each initial pressure head condition. The plots of b and c vs. rainfall intensity are shown in figures 11a and 11b, respectively; the plots of d and e vs. rainfall intensity are shown in figures 12a and 12b, respectively. The respective coefficients for the instantaneous ponding conditions from the case of instantaneous ponding are also shown in these figures, as they represent the limiting values at large intensities, arbitrarily against 100 cm h^{-1} intensity. There is generally a linear decreasing trend for c with respect to increasing rainfall intensity, whereas b decreases asymptotically with increasing rainfall intensity to approach the limiting value. On the other hand, d and e increase logarithmically with intensity to approach the limiting value.

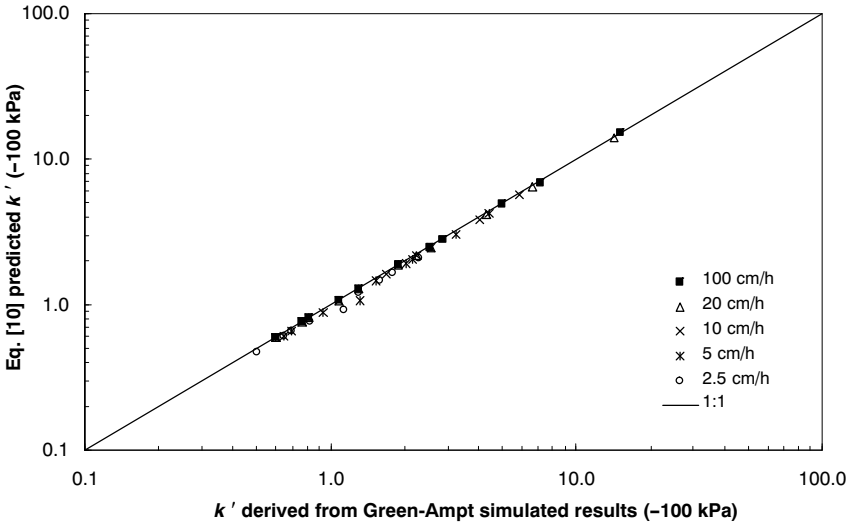

Figure 10. Comparison of equation 10 predicted k' and k' derived from Green-Ampt simulated results for different rainfall intensities and all soils, including instantaneous ponding cases at 100 cm h^{-1} intensity from figure 4.

Table 6. Fitted regression lines relating the extended Lewis-Kostiakov equation parameters α' or k' to the saturated hydraulic conductivity $\overline{K}_s$ for the eleven textural classes at an initial pressure head of –100 kPa and four different rainfall intensities.

	Rainfall Intensity (cm h^{-1})	Regression Equation	r^2
α' versus $\log \overline{K}_s$	2.5	$\alpha = 0.2 \log \overline{K}_s + 0.8234$	0.95
	5.0	$\alpha = 0.1716 \log \overline{K}_s + 0.7502$	0.91
	10.0	$\alpha = 0.1791 \log \overline{K}_s + 0.6539$	0.95
	20.0	$\alpha = 0.1804 \log \overline{K}_s + 0.6281$	0.94
$\log k$ versus $\log \overline{K}_s$	2.5	$\log k = 0.3957 \log \overline{K}_s + 0.2325$	0.97
	5.0	$\log k = 0.4472 \log \overline{K}_s + 0.3228$	0.97
	10.0	$\log k = 0.4619 \log \overline{K}_s + 0.3989$	0.98
	20.0	$\log k = 0.558 \log \overline{K}_s + 0.3965$	0.99

Prediction of Cumulative Infiltration Until Ponding

The I_p for each soil and rainfall intensity was estimated from the equation based on the Green-Ampt approach (eq. 6) with G given by equation 9, assuming that only $\overline{K}_s$ for each soil and θ_s and θ_i were known. The λ values required in equation 9 were obtained from $\overline{K}_s$ by inverting the $\log \overline{K}_s$-$\log \lambda$ linear relationship given in Kozak and Ahuja (2005):

$$\log \lambda = 0.2591 (\log \overline{K}_s) - 0.5825 \qquad (13)$$

This linear equation was used to determine a λ value at each $\overline{K}_s$ value. The subsequent λ values were then used to derive a ψ_b value from the λ-based linear regression equation in Kozak and Ahuja (2005). The λ and ψ_b values were then used to derive a G value according to equation 9. Thus, the G, and indirectly, ψ_b were derived solely from $\overline{K}_s$ and then used in equation 6.

The predicted and G-A simulated I_p values from all scenarios and soils were plotted on a 1:1 graph (–1500 kPa in fig. 13a; –100 kPa in fig. 13b). It was observed that the predicted I_p values were in fair to good agreement with the simulated I_p results. The differences between the predicted and simulated I_p values may be due to error in calculating I_p from the simulated data; larger time steps affect the precision of the simulated I_p determination. Additionally, predicted results are approximations as the $\overline{K}_s$-based λ and ψ_b are employed in equation 6.

Conclusions and Further Discussion

The results of this study lead to the following new contributions to infiltration science and technology:

1. All three parameters (α, k, and t_b) of the original Lewis-Kostiakov equation (eq. 2), and its longer-time extrapolation (eq. 3), for incipient-ponded water infiltration were strongly related to soil $\overline{K}_s$ or λ across the entire range of soil textural classes. This is valuable new knowledge of how infiltration across soil types is explicitly and quantitatively related. The relationships presented allow researchers to quickly estimate all three parameters, and hence infiltration, for each soil type on a landscape or watershed from knowledge of only one parameter, $\overline{K}_s$ or λ. $\overline{K}_s$ can be measured in the field from a simple infiltration study, and either λ or $\overline{K}_s$ can be estimated from soil texture (or particle size distribution) and bulk density. Thus, the spatial distribution of infiltration over a large area can be quickly assessed, and the infiltration estimate scaled up from a small area to a large area based on one parameter for each soil type. The distribution can also be used to estimate an effective average single parameter for lumped modeling of the large area, as commonly done in watershed modeling, which will give the same total infiltration as the sum of individual soils within this area. More detailed models of infiltration can compute infiltration in different soil types based on estimation of all soil hydraulic parameters for each soil, but such models lack this simple approach to scaling and an effective single parameter.

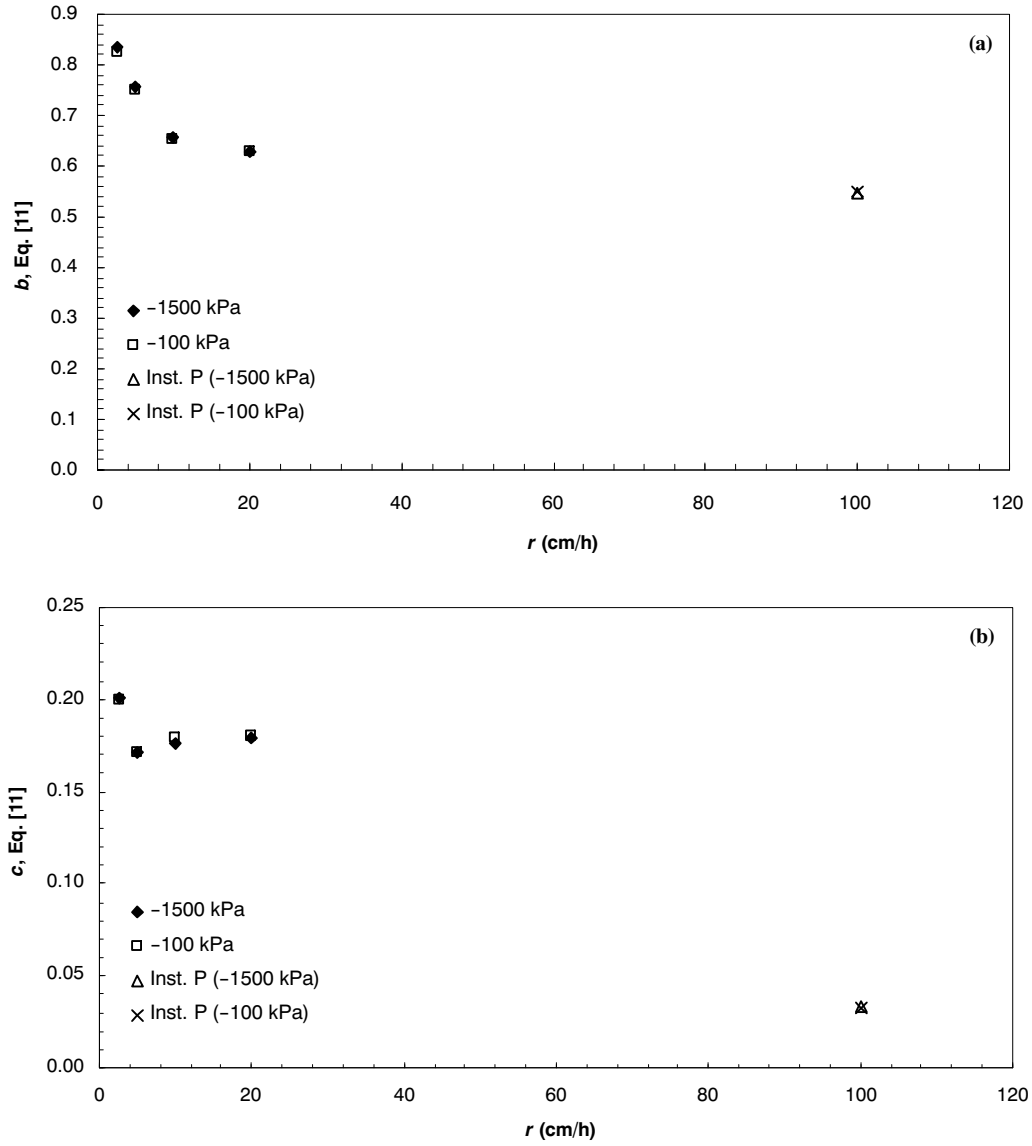

Figure 11. (a) Relationship between the intercept *b* from equation 11 and rainfall intensity for both initial pressure heads, and (b) relationship between the slope *c* from equation 11 and rainfall intensity for both initial pressure heads.

2. This study provides a more physical interpretation of the Lewis-Kostiakov parameters (eqs. 2 and 3) and, heretofore unknown, the effect of initial soil water content or pressure head on the parameters. In a clayey soil, the α value was close to the theoretical value of 0.50 for horizontal infiltration because the gravity effect was negligible for the 5 h duration of infiltration. The α value increased gradually for lighter soil textures, with the value approaching 0.6 for the sand and loamy sand textural classes; this reflected the added effect of gravity. For any given textural class, the α value was about the same for the two initial soil water pressure heads of −1500 and −100 kPa. The *k* values for a given textural class were different at the two pressure heads but were found to be related to each other through equation 10, based on the theoretical relation for sorptivity. This study also shows the validity of the larger-time extension of the L-K equation (eq. 3), thus making it more valuable.

3. An exciting new finding is that the Lewis-Kostiakov equation can be extended to non-instantaneous ponded water infiltration, such as for infiltration of medium- to high-intensity rainfalls (just like the extension of the Green-Ampt infiltration equation). The parameters of this extended equation (k' and α') for each rainfall intensity were again strongly related to the soil $\overline{K}_s$ or λ across the entire range of soil textural classes, providing advantages for estimating spatial distribution and scaling-up of infiltration, as described in paragraph 1 above. The effect of initial soil water pressure head on k' and α' were surprisingly similar to the effects described in paragraph 2 above for the original equation. The variation of the parameters of the α' vs. $\overline{K}_s$ and k' vs. $\overline{K}_s$ relationships with rainfall intensity was also presented, which should be useful for applications.

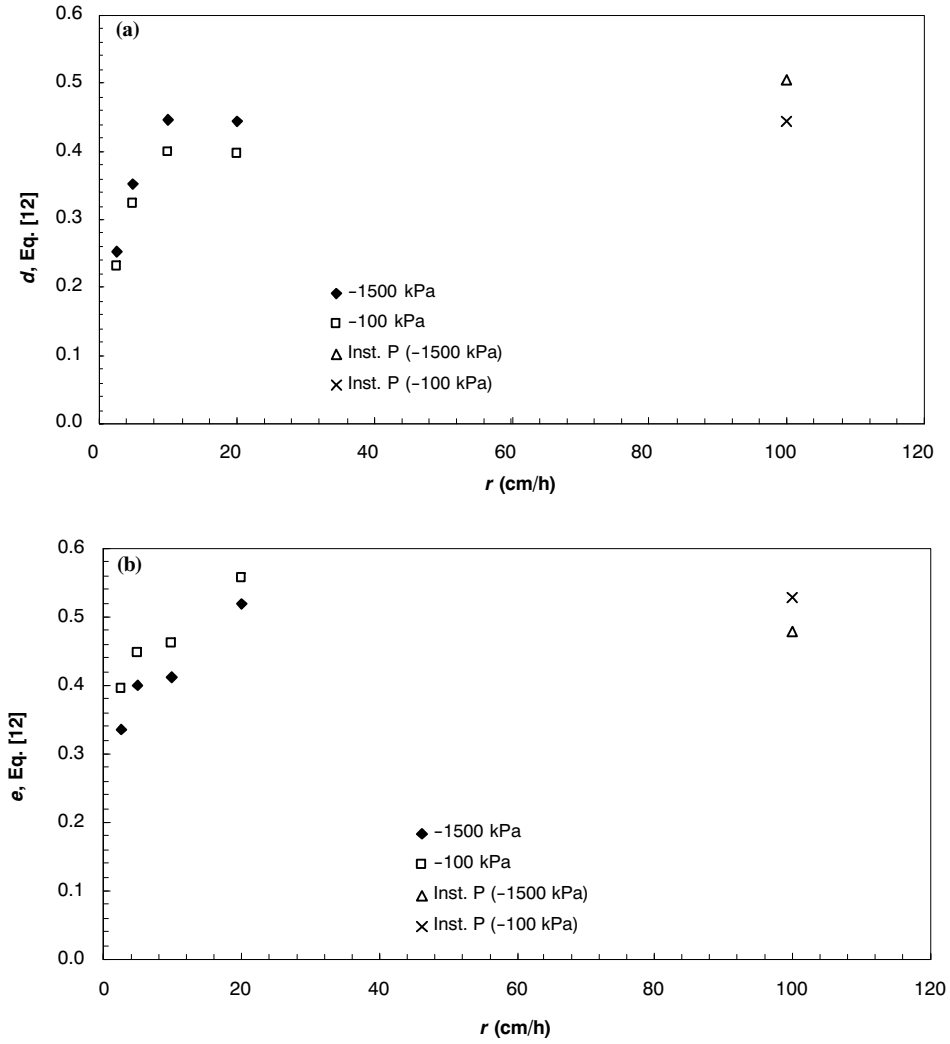

Figure 12. (a) Relationship between the intercept *d* from equation 12 and rainfall intensity for both initial pressure heads, and (b) relationship between the slope *e* from equation 12 and rainfall intensity for both initial pressure heads.

The results of the study are, no doubt, theoretical in the sense that they are based on model-generated data and have not yet been verified against some experimental data. The interesting and useful results presented above are an important first step, and these results should be verified against experimental data in further studies. As described in the Materials and Methods section, the present results are based on the established and accepted Green-Ampt theory, which has been tested and verified extensively against experimental data, both in soil columns and at the field (literature was cited earlier). The Green-Ampt equation has been shown to be physically based and a reasonable simplification of the Richards equation. Furthermore, the Green-Ampt parameters used in the generation of infiltration data were the geometric mean values of measured data for numerous soils across textural classes that were compiled and analyzed by Rawls et al. (1982). Therefore, we believe it was a good use of the above theoretical approach to derive simple relations for scaling infiltration and to study how infiltration across different soil types is related and how the Lewis-Kostiakov parameters are related to one soil parameter and their physical significance. The results have turned out to be extremely valuable. The lack of verification against field data does not diminish the value of these new ideas and knowledge derived from theory. Given that science and knowledge progress in steps, the results of this study are a very good first step towards practical concepts for scaling infiltration and enhancing the value of the simple L-K equation.

In addition, the results presented in this article are for homogeneous soil profiles. It is necessary to examine these empirical relationships with measured data for natural field conditions. In nature, layered soils are a common feature. Can the relationships presented here be employed for these conditions? For most layered soils, one may assume that the parameters of the top 30 cm soil horizon control infiltration. If the top 30 cm of soil is not a uniform horizon, then a harmonic mean of its parameters may be used. Additionally, surface irrigation in the field commonly involves a certain depth of ponding at the soil surface. This ponding depth will increase initial infiltration rates in certain soil types and thus change the Lewis-Kostiakov parameters somewhat. The main effect will be on intercept k of equation 2 (Philip, 1958). For small depths of surface ponding, the increase in k may be assumed linear with depth, and can be estimated from soil properties using the approach of Philip (1958). The k will still, most likely, be related to $\overline{K}_s$. Further research is needed to build upon the simple relationships developed here to incorporate the effects of these additional factors.

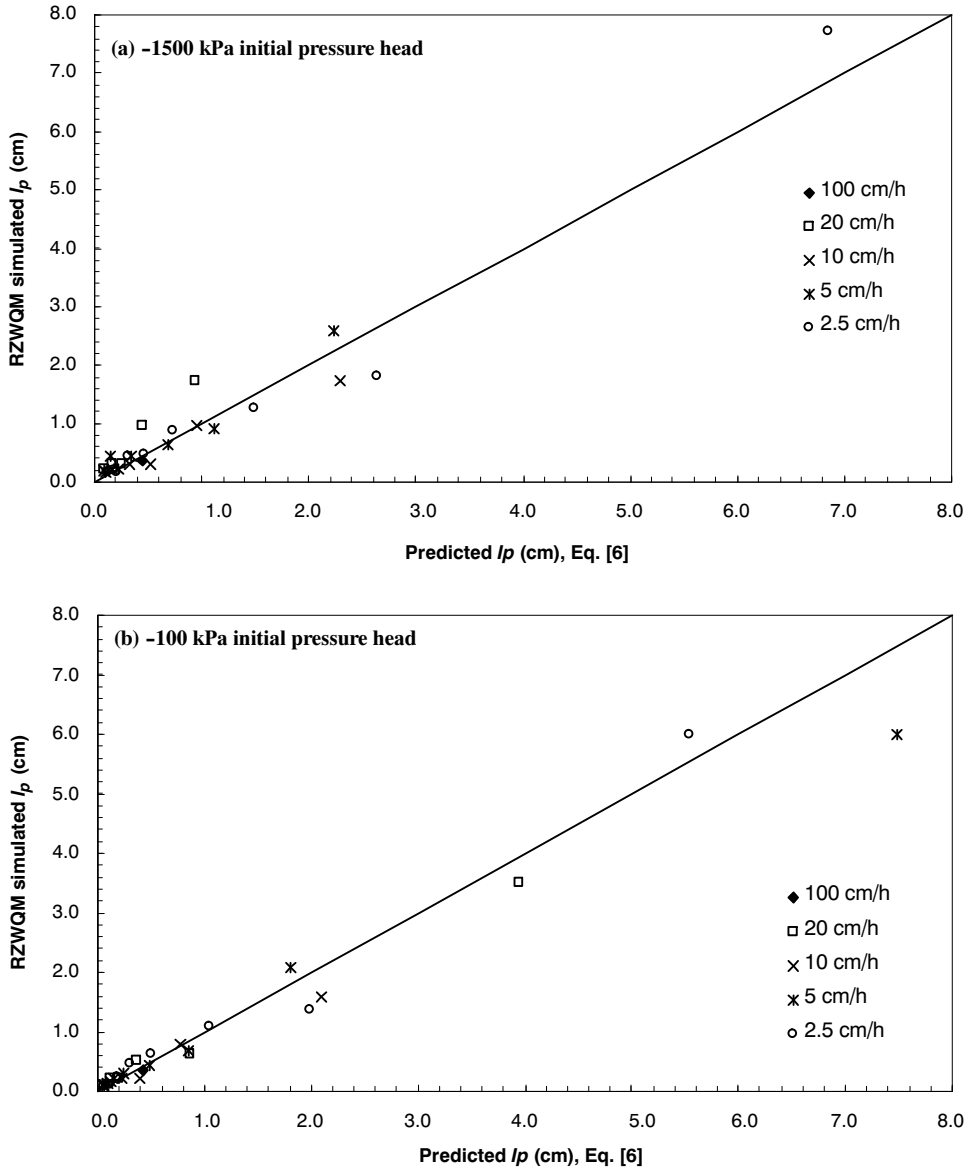

Figure 13. (a) Relationship of predicted I_p and simulated I_p using equation 6 for an initial pressure head of -1500 kPa, and (b) relationship of predicted I_p and simulated I_p using equation 6 for an initial pressure head of -100 kPa.

REFERENCES

Ahuja, L. R. 1983. Modeling infiltration into a crusted soil by the Green-Ampt approach. *SSSA J.* 47(3): 412-418.

Ahuja, L. R., D. G. DeCoursey, B. B. Barnes, ands K. W. Rojas. 1993. Characteristics of macropore transport studied with the ARS Root Zone Water Quality Model. *Trans. ASAE* 36(2): 369-380.

Ahuja. L. R., K. W. Rojas, J. D. Hanson, M. J. Shaffer, and L. Ma, eds. 2000. *Root Zone Water Quality Model: Modeling the Management Effects on Water Quality and Crop Production*. Highland Ranch, Colo.: Water Resources Publications.

ASAE Standards. 2003. EP419: Evaluation of irrigation furrows. St. Joseph, Mich.: ASAE.

Assouline, S. 2005. On the relationships between the pore size distribution index and characteristics of the soil hydraulic functions. *Water Resources Res.* 41(7): 1-8.

Bautista, E., L. Hardy, M. English, and D. Zerihun. 2001. Estimation of soil and crop hydraulic properties for surface irrigation: Theory and practice. ASAE Paper No. 012254. St. Joseph, Mich.: ASAE.

Bouwer, H. 1969. Infiltration of water into non-uniform soil. *J. Irrig. Drain. Div. ASCE* 95(4): 451-462.

Brooks, R. H. and A. T. Corey. 1964. Hydraulic properties of porous media. Hydrological Paper No. 3. Fort Collins, Colo.: Colorado State University.

Cavero, J., E. Playan, N. Zapata, and J. M. Faci. 2001. Simulation of maize grain yield variability within a surface-irrigated field. *Agron. J.* 93(4): 773-782.

Childs, E. C., and M. Bybordi. 1969. The vertical movement of water in stratified porous material: I. Infiltration. *Water Resource Res.* 5(2): 446-459.

Clemmens, A. J. 1981. Evaluation of infiltration measurements for border irrigation. *Agric. Water Mgmt.* 3(4): 251-267.

Clemmens, A. J., D. E. Eisenhauer, and B. L. Maheshwari. 2001. Infiltration and roughness equations for surface irrigation: How form influences estimation. ASAE Paper No. 012255. St. Joseph, Mich.: ASAE.

Colla, G., J. P. Mitchell, B. A. Joyce, L. M. Huyck, W. W. Wallender, S. R. Temple, T. Hsiao, and D. D. Poudel. 2000. Soil physical properties and tomato yield and quality in alternative cropping systems. *Agron. J.* 92(5): 924-932.

Green, W. H., and G. A. Ampt. 1911. Studies of soil physics: 1. Flow of air and water through soils. *J. Agric. Sci.* 4: 1-24.
Hachum, A. Y., and J. F. Alfaro. 1977. Water infiltration and runoff under rain application. *SSSA J.* 41(5): 960-966.
Hunt, A. G., and G. W. Gee. 2002a. Water-retention of fractal soil models using continuum percolation theory. *Vadose Zone J.* 1(2): 252-260.
Hunt, A. G., and G. W. Gee. 2002b. Application of critical analysis to fractal porous media: Comparison with examples from the Hanford site. *Adv. Water. Resour.* 25(2): 129-146.
Idike, F. I., C. L. Larson, D. C. Slack, and R. A. Young. 1980. Experimental evaluation of two infiltration models. *Trans. ASAE* 23(6): 1428-1433.
Kostiakov, A. N. 1932. On the dynamics of the coefficient of water-percolation in soils and on the necessity of studying it from a dynamic point of view for purposes of amelioration. *Trans. 6th Comm. Intl. Soil Science Society* Part A: 17-21.
Kozak, J. A., and L. R. Ahuja. 2005. Scaling of infiltration and redistribution of water across soil textural classes. *SSSA J.* 69(3): 816-827.
Lewis, M. R. 1937. The rate of infiltration of water in irrigation practice. *EOS Trans., American Geophysical Union* 18: 361-368.
Mein, R. G., and C. L. Larson. 1973. Modeling infiltration during a steady rain. *Water Resource Res.* 9(2): 384-394.
Miller, E. E., and R. D. Miller. 1956. Physical theory for capillary flow phenomena. *J. Appl. Phys.* 27(4): 324-332.
Morel-Seytoux, H. J., and J. Khanji. 1974. Derivation of an equation for infiltration. *Water Resource Res.* 10(4): 795-800.
National Research Council. 1991. *Opportunities in the Hydrologic Sciences.* Washington, D.C.: The National Academies Press.
Nielsen, D. R., J. W. Hopmans, and K. Reichardt. 1998. An emerging technology for scaling field soil-water behavior, 136-166. In *Scale Dependence and Scale Invariance in Hydrology.* G. Sposito, ed. Cambridge, U.K.: Cambridge University Press.
NRCS. 1997. Part 652: Irrigation guide. In *National Engineering Handbook.* Washington, D.C.: USDA Natural Resources Conservation Service.
NRCS. 2005. Part 623: Irrigation. Chapter 4: Surface irrigation. In *National Engineering Handbook.* Washington, D.C.: USDA Natural Resources Conservation Service.
Oyonarte, N. A., and L. Mateos. 2002. Accounting for soil variability in the evaluation of furrow irrigation. *Trans. ASAE* 46(1): 85-94.
Pachepsky, Y., D. E. Radcliffe, and H. M. Selim, eds. 2003. *Scaling Methods in Soil Physics.* Boca Raton, Fla.: CRC Press.
Philip, J. R. 1957. Theory of infiltration: 1. The infiltration equation and its solution. *Soil Sci.* 83(5): 345-358.
Philip, J. R. 1958. The theory of infiltration: 6. Effect of water depth over soil. *Soil Sci.* 85(5): 278-286.
Rao, D. M., W. S. Raghuwanshy, and R. Singh. 2006. Development of a physically based 1D-infiltration model for irrigated soils. *Agric. Water Mgmt.* 85(1-2): 165-174.
Rawls, W. J., D. L. Brakensiek, and K. E. Saxton. 1982. Estimation of soil water properties. *Trans. ASAE* 25(5): 1315-1320.
Rieu, M., and G. Sposito. 1991. Fractal fragmentation, soil porosity, and soil water properties: I. Theory. *SSSA J.* 55(5): 1231-1238.
Russo, D., and E. Bresler. 1980. Scaling soil hydraulic properties of a heterogeneous field. *SSSA J.* 44(4): 681-683.
Sharma, M. L., G. A. Gander, and C. G. Hunt. 1980. Spatial variability of infiltration in a watershed. *J. Hydrol.* 45(1-2): 101-122.
Simmons, C. S., D. R. Nielsen, and J. W. Biggar. 1979. Scaling of field-measured soil water properties. *Hilgardia* 47(4): 77-154.
Smith, R. E. 2002. Infiltrability models: Comparisons and application. In *Infiltration Theory for Hydrologic Applications*, 97-118. K. R. J. Smettem, P. Broadbridge, and D. A. Woolhiser, eds. Washington D.C.: American Geophysical Union.
Swartzendruber, D. 1993. Revised attribution of the power form infiltration equation. *Water Resource Res.* 29(7): 2455-2456.
Swartzendruber, D., and M. R. Huberty. 1958. Use of infiltration equation parameters to evaluate infiltration differences in the field. *Trans. American Geophys. Union* 39: 84-93.
Tillotson, P. M., and D. R. Nielsen. 1984. Scale factors in soil science. *SSSA J.* 48(5): 953-959.
Tyler, S. W., and S. W. Wheatcraft. 1990. Fractal processes in soil water retention. *Water Resource Res.* 26(5): 1047-1054.
Walker, W. R., and G. V. Skogerboe. 1987. *Surface Irrigation: Theory and Practice.* Englewood Cliffs, N.J.: Prentice-Hall.
Warrick, A. W., G. M. Mullen, and D. R. Nielsen. 1977. Scaling field-measured soil hydraulic properties using a similar-media concept. *Water Resource Res.* 13(2): 355-362.
Williams, R. D., and L. R. Ahuja. 2003. Scaling and estimating the soil water characteristic using a one-parameter model. In *Scaling Methods in Soil Physics*, 35-48. Y. Pachepsky, D. E. Radcliffe, and H. M. Salim, eds. Boca Raton, Fla.: CRC Press.
Wilson, B. N., D. C. Slack, and R. A. Young. 1982. A comparison of three infiltration models. *Trans. ASAE* 25(2): 349-356.